Zhao *et al.*
Chinese Journal of Mechanical Engineering (2024) 37:84
https://doi.org/10.1186/s10033-024-01071-z

Chinese Journal of Mechanical Engineering

ORIGINAL ARTICLE

Open Access

Multi-Objective Optimization of the Ultrasonic Scalpel Rod and Tip with Improved Performance: Vibration Frequency, Amplitude, and Service Life

Jiaqi Zhao[1], Yuhao Zhai[1], Xuzhe Jia[1], Naiwen Deng[1], Kunxu Li[1], Guangchao Han[1,2], Rong Chen[1,2], Dong Wang[3] and Wei Bai[1,2,4*]

Abstract

Ultrasonic scalpel design for minimally invasive surgical procedures is mainly focused on optimizing cutting performance. However, an important issue is the low fatigue life of traditional ultrasonic scalpels, which affects their long-term reliability and effectiveness and creates hidden dangers for surgery. In this study, a multi-objective optimal design for the cutting performance and fatigue life of ultrasonic scalpels was proposed using finite element analysis and fatigue simulation. The optimal design parameters of resonance frequency and amplitude were determined. By setting the transition fillet and keeping the gain structure away from the node position to enable the scalpel to have a high service life with excellent cutting performance. The frequency modulation method of setting the vibration node bosses at the node position and setting the vibration antinode grooves at the antinode position was compared. Then, the mechanism of the influence of various design elements, such as tip, shank, node position, and antinode position, on the resonance frequency, amplitude, and fatigue life of the ultrasonic scalpel was analyzed, and the optimal design principles of the ultrasonic scalpel were obtained. The proposed ultrasonic scalpel design was confirmed by simulations, impedance measurements, and liver tissue cutting experiments, demonstrating its feasibility and enhanced performance. This research introduces innovative design strategies to improve the fatigue life and performance of ultrasonic scalpels to address an important issue in minimally invasive surgery.

Keywords Multi-objective optimal design, Minimally invasive surgical procedures, Service life, Ultrasonic scalpel

1 Introduction

Ultrasonic scalpel [1] is becoming a revolutionary innovation in minimally invasive surgery due to its excellent cutting and coagulation effects. Compared with electric scalpels and laser scalpels [2, 3], ultrasonic scalpels have many advantages such as less adhesion with tissues, less smoke, less postoperative scarring, and fewer postoperative complications [4], and it has been widely used in endoscopic surgery [5, 6]. Ultrasonic scalpel system is usually composed of ultrasonic transducer, ultrasonic scalpel rod, and tip. As shown in Figure 1, the ultrasonic transducer converts the ultrasonic electric energy generated by the power supply into ultrasonic vibration [7, 8],

*Correspondence:
Wei Bai
wbai@cug.edu.cn
[1] School of Mechanical Engineering and Electronic Information, China University of Geosciences, Wuhan 430074, China
[2] Shenzhen Research Institute, China University of Geosciences, Shenzhen 518057, China
[3] College of Engineering, Mathematics and Physical Sciences, University of Exeter, Exeter EX4 4QF, UK
[4] Shenzhen Huazhong University of Science and Technology Research Institute, Shenzhen 518000, China

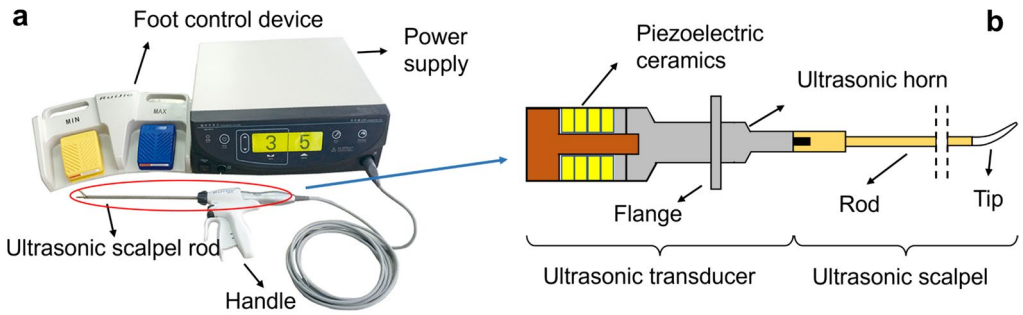

Figure 1 Ultrasonic Scalpel System: (**a**) Composition of the GEN100 Ultrasonic Scalpel System, (**b**) Structural diagram of ultrasonic scalpel

and amplifies the ultrasonic amplitude through the ultrasonic horn. The ultrasonic scalpel rod further transmits the ultrasonic vibration to the tip to complete the cutting and coagulation of body tissues, so as to meet the purpose of treatment [9, 10].

Ultrasonic scalpels need a stable resonance frequency to provide the required amplitude for cutting and coagulating closed target tissues during the working process [11, 12]. Therefore, the resonant frequency and output amplitude of the ultrasonic scalpel are essential performance indicators in the design process of the ultrasonic scalpel. Ultrasonic scalpels will be excited by ultra-high frequency loads during work, and the tip of the ultrasonic scalpels is prone to extremely high-cycle fatigue fractures [13]. To reduce the probability of medical accidents caused by breakage of ultrasonic scalpel tip, the ultrasonic scalpel is generally a disposable medical supply in clinical use, which not only wastes materials but also increases the burden on patients. Therefore, fatigue life is also a very important performance indicator in the design of ultrasonic scalpels.

Researchers in this field have been committed to developing ultrasonic scalpels with higher performance. Umehara et al. [14] developed a miniature transducer, 9.8 mm long and 2.7 mm wide, which can be matched with the endoscope, improving the surgical field of vision and the doctor's operating space. Wiksell et al. [15] proposed a modeling method, which can simulate and automatically adjust each interactive part of the design before actual manufacturing, thus reducing the iteration difficulty in the design process of the miniature ultrasonic scalpel. Li et al. [16] proposed an ultrasonic scalpel based on longitudinal and torsional modes with better hemostatic ability, which improved the energy used to seal blood vessels. Ethicon [17] developed a new type of hemostatic ultrasonic scalpel Harmonic ACE ®+ 7 Shears (Harmonic 7) can seal thick blood vessels by reducing the input power during cutting, which can achieve hemostasis and closure of 5 mm thick blood vessels. THUNDERBEAT ™ (Olympus, Japan) [18] combines the friction heat generated by ultrasound and the heat generated by piezoelectric to work, with higher versatility, similar fracture pressure, and acceptable thermal diffusion. The above researches mainly focus on improving the cutting performance and hemostatic performance of the ultrasonic scalpel.

The fatigue performance [19, 20] of the ultrasonic scalpel is also an important index to evaluate the performance of the ultrasonic scalpel. Ultrasonic fatigue refers to the fatigue damage of materials under ultrasonic vibration load, which has the characteristics of small vibration amplitude, high cycle times, and short duration. The fatigue research of ultrasonic scalpel belongs to the category of ultrasonic fatigue and has been studied by many researchers. Tjong et al. [21] studied the microstructure and fracture of aluminum alloys and aluminum alloy composites using fatigue test techniques and demonstrated their fatigue behavior, paving the way for the widespread application of titanium alloys in the manufacture of ultrasonic scalpels. Stanzl et al. [22] applied shear stress to the sample and carried out ultrasonic torsional vibration fatigue tests to explore the ultra-high cycle fatigue characteristics of light alloys under different environmental conditions. Lucas et al. [23] established the finite element model and fracture model of ultrasonic cutting, so that the ultrasonic cutting system suitable for the surgical field can be designed. For the fatigue design of structural members, the allowable stress can usually be determined according to the fatigue life curve (S-N curve) of materials and a safety factor. However, for different materials, the distribution of fatigue life in the ultra-high cycle fatigue cycle range is very complex, and many scholars have started to predict fatigue life. Bathias et al. [24] established a high-strength steel ultra-high cycle fatigue life prediction model and a crack growth

threshold calculation model. Ebara et al. [25] modified the fatigue life prediction model by introducing the concept of optical shadowing area (ODA) based on a large number of experimental studies. Li et al. [26] studied the high cycle fatigue performance of Ti6Al4V, conducted axial loading tests with variable stress ratio, obtained S-N curves of Ti6Al4V under different stress ratio conditions, and proposed a life prediction method related to failure mechanism. Research has shown that the fatigue life of ultrasound knives is strongly correlated with the stress of the structure [27]. Zhang et al. [28] used nCode software to study the fatigue life of a torsion beam of a certain car, and obtained the stress distribution and fatigue life of the beam structure. This method can provide the basis for the optimal design of the torsion beam. Cao et al. [29] studied the influence of the blade and blade structure of ultrasonic scalpels on frequency and stress, summarized the changes in stress, and optimized the frequency and fatigue life of ultrasonic scalpels based on this. Chen et al. [30] used harmonic response analysis to calculate the tip amplitude, impedance, and stress distribution of ultrasound bone knives, and optimized the error using response surface methodology. They summarized optimization methods for reducing the stress of ultrasound bone knives. Li et al. [31] optimized the design of ultrasonic scalpels based on finite element method and developed a low stress, high service life ultrasonic scalpel. It is worth noting that currently few scholars have incorporated fatigue life as a direct technical indicator into the design and optimization process of ultrasound scalpels.

At present, established methods can accurately predict the ultra-high cycle fatigue life of high–strength materials. However, predicting the fatigue life of the ultrasonic scalpel, which has a complex structure and dispersed internal stress, requires an appropriate prediction model and continuous fatigue iterative simulation. In this study, the authors conduct a comprehensive investigation of the influence of structural parameters of the ultrasonic scalpel rod and tip on the resonance frequency, amplitude, and fatigue life of the device through a combination of simulation and experimental verification. The authors present an optimal structure design method for the ultrasonic scalpel within a certain range, which enables the creation of an ultrasonic scalpel with high performance and improved fatigue life.

2 Mechanical Design of the Ultrasonic Scalpel

2.1 Preliminary Structural Design of Rod

The ultrasonic scalpel design starts from an equal-sectional thin rod [32]. According to the propagation theorem of sound waves, when ultrasonic waves propagate in a thin rod, they will reflect and form a reflected wave after contacting the end surface, and the reflected wave and incident wave will form a standing wave through interference [33, 34]. The place with the largest amplitude of the waveform is called the antinode, and the place with the smallest amplitude is called the node [35, 36]. The standing wave equation is:

$$\xi(t,x) = (A\cos kx + B\sin kx)\cos(\omega t - \varphi), \tag{1}$$

and

$$k = \omega/c, \tag{2}$$

where, $\xi(t,x)$ represents the displacement at the time t and x coordinate. A and B are the undetermined coefficient, k is the wave number, ω is the frequency, $\cos(\omega t - \varphi)$ is the phase, and φ is the initial phase angle, which does not affect the calculation result. The process of ultrasonic scalpel withstanding transducer excitation is simplified as that of the thin rod withstanding simple harmonic force, as shown in Figure 2(a). According to the longitudinal vibration law of the thin rod, the boundary condition of the ultrasonic scalpel with one end free and one end bearing simple harmonic force is as follows:

$$\begin{cases} \dfrac{\partial \xi}{\partial x}|_{x=0} = 0, \\ F_{\max}\cos(\omega t - \varphi) = -SE\dfrac{\partial \xi}{\partial x}|_{x=l} = 0, \end{cases} \tag{3}$$

where, S is the diameter of the thin rod, E is the elastic modulus, l is the total length of the rod, and the negative sign indicates that the direction of stress and strain is opposite, $F_{\max}$ is the maximum value of simple harmonic force. Combining the above equation with the acoustic wave propagation characteristics, the vibration characteristic equation of the thin rod with one end free and one end bearing simple harmonic force is calculated:

$$\xi(t,x) = \frac{F_{\max}}{SEk\sin kl}\cos kx\cos(\omega t - \varphi), \tag{4}$$

where, $\xi(t,x)$ is positively correlated with $F_{\max}$, it proves that the vibration displacement of the thin rod increases with the increase of the force. When the frequency of the simple harmonic force is equal to the natural frequency of the thin rod, the amplitude of the thin rod will reach the maximum. The position equations of antinodes and nodes of the thin rod are obtained as follows:

$$\begin{cases} x_{ncodes} = (2y-1)\dfrac{\lambda_n}{4} = \dfrac{2y-1}{2n}l\ (y = 1,2,3\ldots), \\ x_{antinodes} = 2\,(y-1)\dfrac{\lambda_n}{4} = \dfrac{2(y-1)}{2n}l\ (y = 1,2,3\ldots), \end{cases} \tag{5}$$

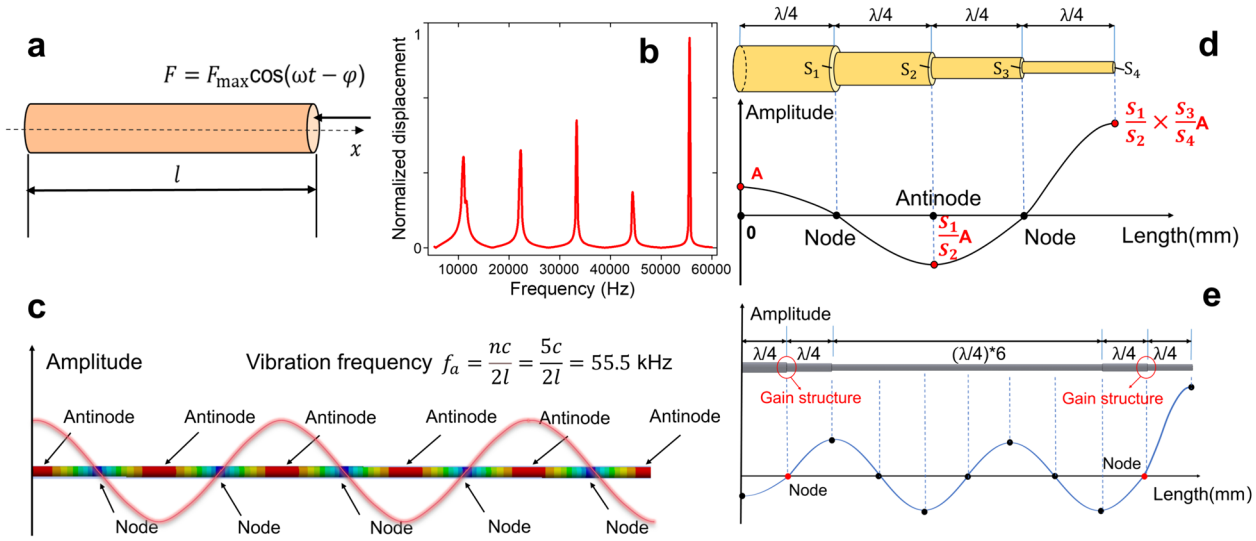

Figure 2 Design of resonance frequency and amplitude gain for ultrasonic scalpel: (**a**) Thin rod with one end bearing simple harmonic force and one end free, (**b**) Resonant frequency, (**c**) Deformation results of the thin rod at 55 kHz, (**d**) Amplitude amplification mechanism of the stepped rod, (**e**) Amplitude gain design of ultrasonic scalpel

and

$$f_n = \frac{nc}{2l}(n = 1, 2, 3...), \tag{6}$$

$$\lambda_n = \frac{c}{f_n}(n = 1, 2, 3...), \tag{7}$$

where, c is the ultrasonic propagation velocity, λ_n is the wavelength, f_n is the longitudinal vibration frequency of the thin rod, when $n = 1$, f_1 is the fundamental frequency, and other longitudinal frequencies are positive integral multiples of the fundamental frequency, which is called overtones. Eq. (5) shows that for a thin rod with one end free and one end bearing simple harmonic force, the nodes are at an odd number of times of the quarter wavelength, and the antinodes are at an even number of times of the quarter wavelength. And the positions of nodes and antinodes are related to the total length l of the thin rod. Therefore, to minimize the impact of changes in the positions of the nodes and antinodes on the rod, the total length l of the rod should be kept as constant as possible during the design process.

The ultrasonic scalpel undergoes ultra-high cycle load excitation during operation, making it very prone to fatigue fracture. To make it more suitable for surgical operation, materials with good ductility, portability, and fatigue resistance should be selected, with small loss and impedance within the operating frequency range. Considering these factors, the authors selected TC4 [37, 38] as the material for the ultrasonic scalpel. The ultrasonic propagation velocity c in TC4 is 4944 m/s [39]. Eq. (7) shows that product of λ_n and f_n remains constant. The resonance frequency of the ultrasonic scalpel designed in this study is 55.5 kHz, so the wavelength λ is determined as 89 mm. According to the ultrasonic vibration characteristics of the thin rod [33], when the total length of the thin rod is half wavelength $\lambda/2$, the thin rod meets the condition of longitudinal vibration. To provide a larger surgical field of vision and meet the needs of surgery, the authors preset the total length of the ultrasonic scalpel l as 2.5 wavelengths, or 223 mm.

A three-dimensional structure of a thin rod made of TC4 material with a length of 223 mm was modeled, and the calculation results were verified using model analysis, as depicted in Figure 2(b). The fundamental frequency f_1 is 11.1 kHz and the design frequency f_5 is 55.5 kHz. After comparing the calculated results with Eqs. (1), (5), it was determined that the frequency response results obtained from the simulation were in perfect agreement with the theoretical frequency equations. Moreover, the simulation results shown in Figure 2(c) (in the case where the frequency f_a is 55.5 kHz) showed that when the thin rod is at the longitudinal vibration frequency, the positions of nodes and antinodes were entirely consistent with the theoretical calculation. Figure 2(b) shows that when the frequency was around 55.5 kHz, the thin rod had better displacement. The research has shown that the ultrasonic scalpel had good cutting performance when the resonant frequency was around 55.5 ± 1 kHz. Therefore, the design frequency of the ultrasonic scalpel in this study was set between 54.5 kHz–56.5 kHz.

The research shows that when the frequency is 55.5 kHz, the output amplitude of the ultrasonic scalpel

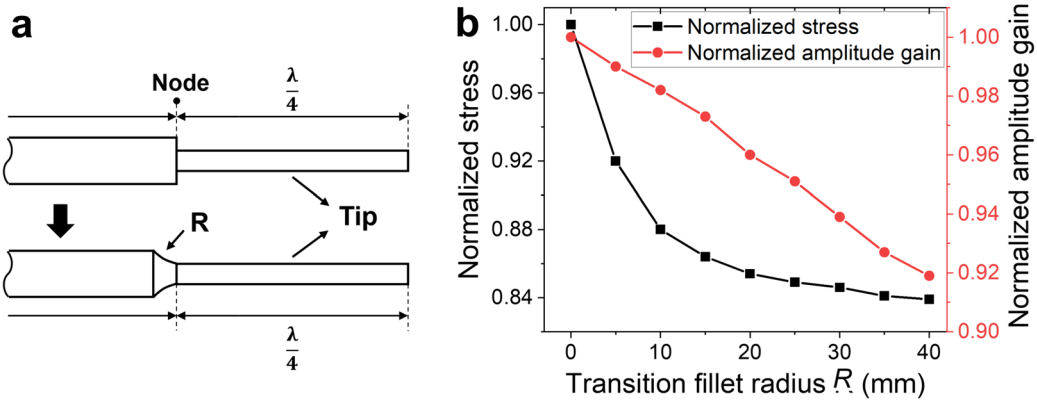

Figure 3 Settings for transition fillets: (**a**) Position of transition fillets, (**b**) Effect of transition fillet radius on stress and amplitude gain

tip should reach 41 μm above and can meet the conditions of soft tissue cutting [39]. The input amplitude of the ultrasonic scalpel is generally about 10 μm [40]. To make the output amplitude of the ultrasonic scalpel meet the cutting requirements, the input amplitude of the ultrasonic scalpel needs to be amplified. This paper uses the FEM method to simulate the amplitude amplification mechanism of a thin rod, as shown in Figure 2(d), when the shaft segment with a small diameter is at the node position of the thin rod, the amplitude gain can be obtained, and the gain value is the ratio of the sectional areas of the two shaft segments. When the shaft segment with a small diameter is at the antinode position of the thin rod, the amplitude will not change. On this basis, the structure of the ultrasonic scalpel rod is designed, as shown in Figure 2(e). Two amplitude gain structures were designed near the node positions at both ends of the rod. It is worth noting that this setup method avoids the stress concentration caused by the abrupt structural change induced by setting up only one gain structure, thereby improving the service life of the ultrasonic scalpel. The middle region of the rod is usually not equipped with a gain structure to maintain the stability of ultrasound transmission and improve the efficiency of ultrasound transmission.

2.2 Optimization Design of Ultrasonic Scalpel Tip

The main clinical functions of the ultrasonic scalpel tip include cutting, coagulation, tissue separation, clamping. Traditional ultrasonic scalpels are limited by the problems of short length and small curvature, which always lead to insufficient surgical space, and the low service life of the tip is always a surgical risk. To solve these problems, a proposed design for an ultrasonic scalpel with a larger radian, longer and thinner distal tip is introduced in this study, providing a larger surgical field of view compared to traditional ultrasonic scalpels. The proposed ultrasonic scalpel tip is located in the last half wavelength of the ultrasonic scalpel rod, and includes a gain structure and a cutting end tip. By extending the tip length, increasing the curvature of the cutting end and reducing the tip diameter, the ultrasonic scalpel not only provides a larger operating space and reduces the difficulty for the surgeon, but also extends the life of the ultrasonic scalpel while maintaining a very good cutting amplitude. In addition, the reduced cutting surface facilitates the cutting of soft tissue.

To increase the amplitude, researchers typically place a variable-section gain structure at the node position near the tip. However, due to the serious stress concentration caused by the change of section, fatigue damage is very easy to occur. At present, it is still difficult to achieve accurate prediction and failure warning of the fatigue fracture time of the tip. Therefore, to reduce the risk of surgical accidents, it is necessary to reduce the stress on the structure of this position and prolong the time of the ultrasonic scalpel. The simple way to improve stress concentration is to add transition fillet radius at the gain structure, as shown in Figure 3(a). But setting transition fillet radius at the node position will undoubtedly have an adverse effect on the vibration amplitude of the tip. To minimize the stress amplitude and make the amplitude gain meet the cutting requirements of the ultrasonic scalpel, it is necessary to analyze the size of the transition fillet radius R. Taking different transition fillet radius R, the influence of transition fillet radius R on the stress and amplitude gain of the ultrasonic scalpel is obtained through finite element analysis, as shown in Figure 3(b). In the range of the transition fillet radius R of 0–40 mm, the stress decreases with the increase of R, but the rate of stress decrease gradually slows down, and the amplitude gain decreases gradually with the increase of R. When R

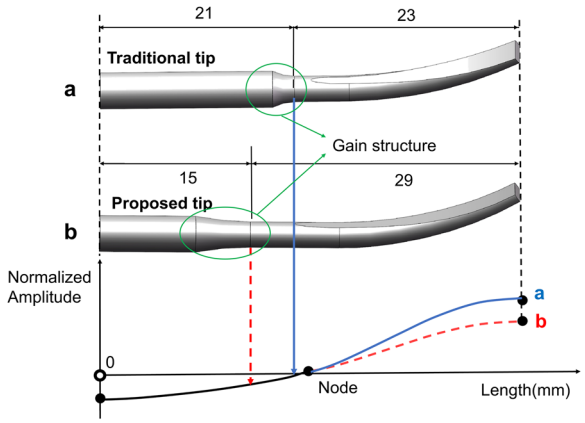

Figure 4 (**a**) Traditional ultrasonic scalpel tip and (**b**) proposed ultrasonic scalpel tip that makes the connection between the tip and the gain structure far away from the node position

Table 1 Performance comparison between proposed and traditional ultrasonic scalpel

Parameters	Traditional tip	Proposed tip
Resonant frequency (kHz)	55.961	55.510
Number of cycles	5.483×10^8	1.772×10^9
Fatigue life (h)	81	241.5
Average amplitude (μm)	78	65

is in the range of 0–20 mm, the stress decreased by about 14.6%, and the amplitude decreased by about 4.1%, and when R is in the range of 20–40 mm, the stress decreased by about 1.5%, and the amplitude decreased by about 4.2%. To minimize the stress concentration of this variable section and make the rod have a larger amplitude gain, the transition fillet radius R should be selected between 10–20 mm.

This paper proposes another method to reduce stress concentration and improve fatigue life, as shown in Figure 4. The tip is improved by extending the length of the tip to move the gain structure away from the node location.

The results of model analysis of traditional tip and proposed tip are shown in Table 1. The optimization of the ultrasonic tip significantly improves the fatigue life from 81 h to 241.5 h. It should be noted that the process of calculating the life of the ultrasonic scalpel in this study is the case of no load of the ultrasonic scalpel (no touching the soft tissue). Although the output amplitude is reduced to a certain extent, the amplitude fully meets the cutting requirements, and this design is completely feasible.

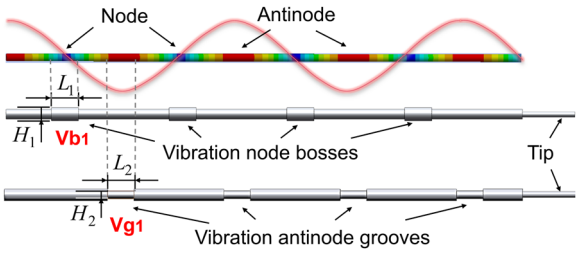

Figure 5 Position of the VN bosses and VA grooves of the ultrasonic scalpel

The above method prolongs the service life of the ultrasonic scalpel and improves the performance of the ultrasonic scalpel.

3 Multi–Objective Optimization Design Based on Model Analysis and Fatigue Simulation

After conducting initial theoretical calculations, this paper uses ANSYS and nCode DesignLife software to simulate the ultrasonic scalpel. The simulation analyzes how various structural parameters affect the scalpel's frequency, amplitude, and fatigue life. By optimizing the mechanical structure based on these results, this study successfully enhances the performance of the ultrasonic scalpel.

3.1 Optimal Design of Vibration Node Bosses

In the engineering manufacturing process of ultrasonic scalpel, factors like machining accuracy, manufacturing assembly errors, and material properties affect the resonant frequency of the device and cause deviations from the design value. Typically, for a thin rod, the frequency can be calibrated by reserving a length of process tolerance at the end. However, due to the long and highly curved shape of the ultrasonic scalpel tip, this process is not feasible.

The ultrasonic scalpel operates by transmitting and amplifying ultrasonic waves generated by the transducer. For optimal performance, the resonant frequency of the scalpel and the transducer should closely match. The frequency of the transducer is 55.5 kHz. To adjust the frequency of the ultrasonic scalpel, this paper proposes a method shown in Figure 5, which involves adding vibration node bosses (VN bosses) at the nodes and vibration antinode grooves (VA grooves) at the antinodes. The addition of VN bosses reduces the radial amplitude of the rod, optimizes the vibration mode, and adjusts the resonant frequency of the ultrasonic scalpel. Similarly, the addition of VA grooves has a similar effect. As long as the central position of these shaft segments coincides with the position of nodes or antinodes, they will not affect

the amplitude of the ultrasonic scalpel. Therefore, the resonant frequency of an ultrasonic scalpel can be calibrated by adjusting the length L_1, diameter H_1, and the number of VN bosses or the length L_2, diameter H_2, and the number of VA grooves. To investigate the influence of the shaft parameters on the ultrasonic scalpel, a three-dimensional model was established and analyzed, the results are shown in Figure 6. For the purpose of analysis, only the parameters of the first VN bosses Vb_1 and the first VA grooves Vg_1 are varied in analyzing the diameter and length of the shaft segments, as shown in Figure 5. The initial diameter of the thin rod is set to 3 mm.

As shown in Figure 6(a), the resonant frequency of the rod increases as the diameter of the VN bosses increases, whereas the resonant frequency decreases with an increase in the diameter of the VA grooves. In Figure 6(b) and (c), when the diameter of the shaft segment exceeds the original diameter of the rod, the resonant frequency of the rod rises with an increase in the length of VN bosses, but decreases with an increase in the length of VA grooves. And if the diameter of the shaft segment is less than the original diameter of the rod, the opposite conclusion is reached. Comparison reveals that the diameter of the shaft segment has a more significant influence on the resonant frequency than its length. Figure 6(d) and (e) show that as the number of VN bosses increases, the resonant frequency of the rod increases when the diameter of the VN bosses are larger than the diameter of the rod, while the resonant frequency of the rod decreases when the diameter of the VN bosses are smaller than the diameter of the rod. For the VA grooves, the conclusion is opposite. In summary, the variation of the diameter of the shaft segment has a greater effect on the resonant frequency than the variation of its length, and the variation of the shaft segment at the nodes and the antinodes has an opposite effect on the resonant frequency of the rod.

Using the same analytical approach, the effect of structure on the fatigue life of the rod was evaluated, and the results are presented in Figure 7. The fatigue life of the rod increases with an increase in the diameter of the shaft segment. When the diameter of the shaft segment exceeds the original diameter of the rod, the fatigue life of the rod can be improved by increasing the number and diameter of shaft segments, irrespective of their location. Conversely, if the diameter of the shaft segment is smaller than the original diameter of the rod, the conclusion is opposite. The impact of the shaft segment diameter on the fatigue life of the rod is greater than the number and length of shaft segments. Thus, changes in the shaft segment at the nodes and antinodes have opposite effects on the resonant frequency of the rod, but their impact on

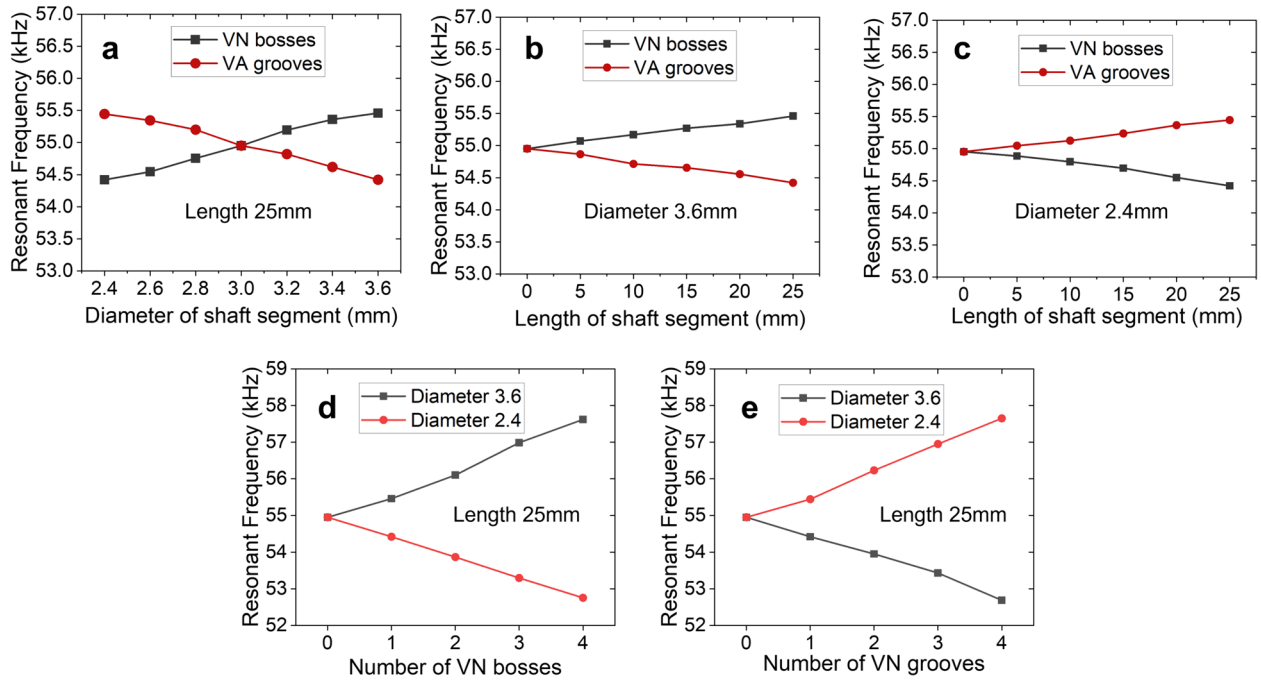

Figure 6 Mechanism of influence of axial structure parameters on the resonant frequency of ultrasonic scalpel: (**a**) Influence of the diameter of shaft segment on the resonance frequency, (**b**) Influence of the length of shaft segment on resonance frequency when the diameter is larger than the rod diameter, (**c**) Influence of the length of shaft segment on resonance frequency when the diameter is smaller than the rod diameter, (**d**) Influence of the number of the VN bosses on the resonance frequency, (**e**) Influence of the number of the VA grooves on the resonance frequency

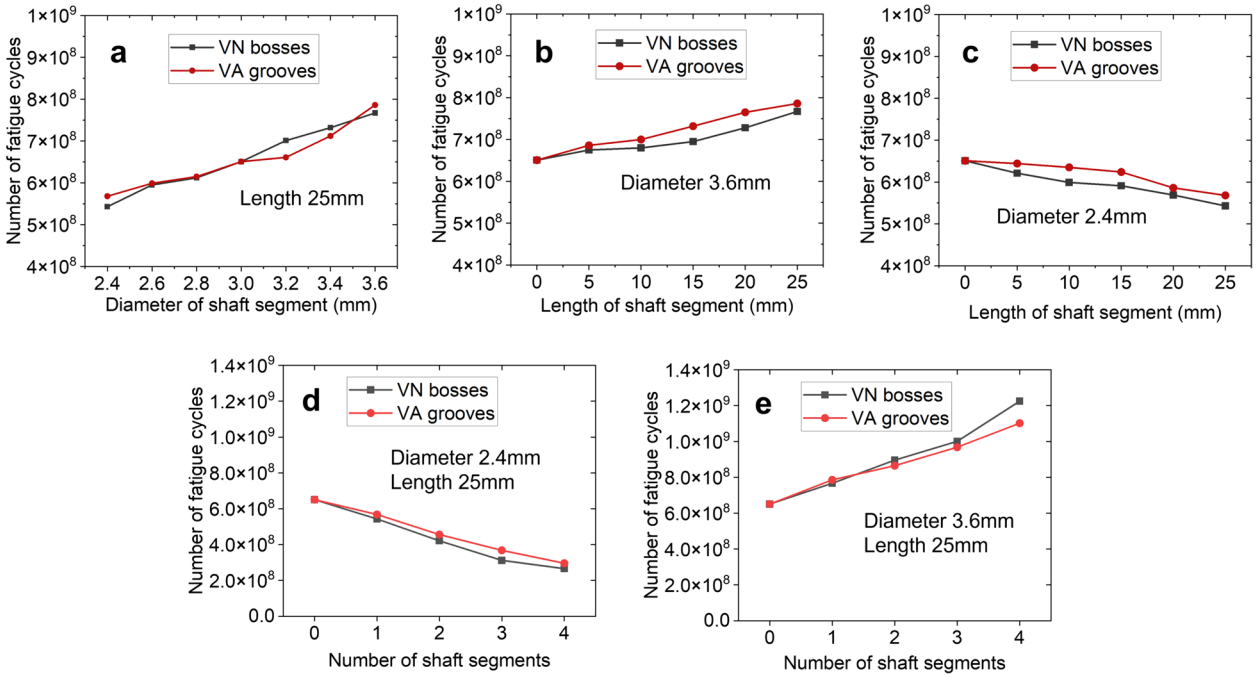

Figure 7 Mechanism of the influence of structural parameters of shaft segment on fatigue life of ultrasonic scalpel: (**a**) Influence of the diameter of the shaft segment on the fatigue life, (**b**) Influence of the length of shaft segment with a diameter greater than the rod diameter on fatigue life, (**c**) Influence of the length of shaft segment with a diameter smaller than the rod diameter on fatigue life, (**d**) Influence of the number of shaft segments with a diameter smaller than the rod diameter on fatigue life, (**e**) Influence of the number of shaft segments with a diameter greater than the rod diameter on fatigue life

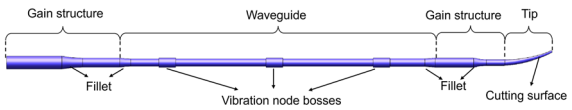

Figure 8 Designed ultrasonic scalpel

the fatigue life of the rod is consistent. Furthermore, the fatigue life of the rod is predominantly associated with its diameter. Therefore, the addition of VN bosses and VA grooves can modulate the resonant frequency, but adding VN bosses improves the fatigue life. Therefore, this design uses the method of adding VN bosses. These findings can also be applied to achieve multi-objective optimization of the ultrasonic scalpel.

3.2 Model Simulation and Fatigue Simulation of Ultrasonic Scalpel

By combining the ultrasonic scalpel design model and the multi–objective optimization design method mentioned earlier, the design structure of the ultrasonic scalpel is shown in Figure 8, with added fillets and internal threaded holes. To study the static and dynamic performance of the ultrasonic scalpel, modal analysis using the finite element method was conducted, as shown in Figure 9. The ultrasonic scalpel demonstrated good longitudinal vibration mode at the 62nd mode with a value of 54910 Hz, which is in line with the working direction of the ultrasonic scalpel and within the preset frequency range of 45–65 kHz, meeting the design requirements. The axial and radial deformation results of the ultrasonic scalpel under the working frequency were extracted, as shown in Figure 9(b) and (c), respectively. The maximum axial and radial deformation ratio is about 45.5, proving that the rod has excellent longitudinal vibration characteristics.

The fatigue life of the ultrasonic scalpel can be predicted by using the transient structural module of ANSYS Workbench and nCode SN Timestep (Designlife) module of the nCode Designlife. Transient structural analysis is a method used to analyze the dynamic response of structures caused by time-varying excitation in a very short time. The ultrasonic scalpel in this study was subjected to a sinusoidal force excitation with a fixed amplitude, and the working life was calculated by analyzing the influence of displacement load on the strain stress over time. The resonant frequency of the designed ultrasonic scalpel is 54910 Hz, with 54910 cycles performed within 1 s. The time of each sine wave cycle, that is, the time of one cycle of the sine wave cycle, is 1.81×10^{-5} s. The total length

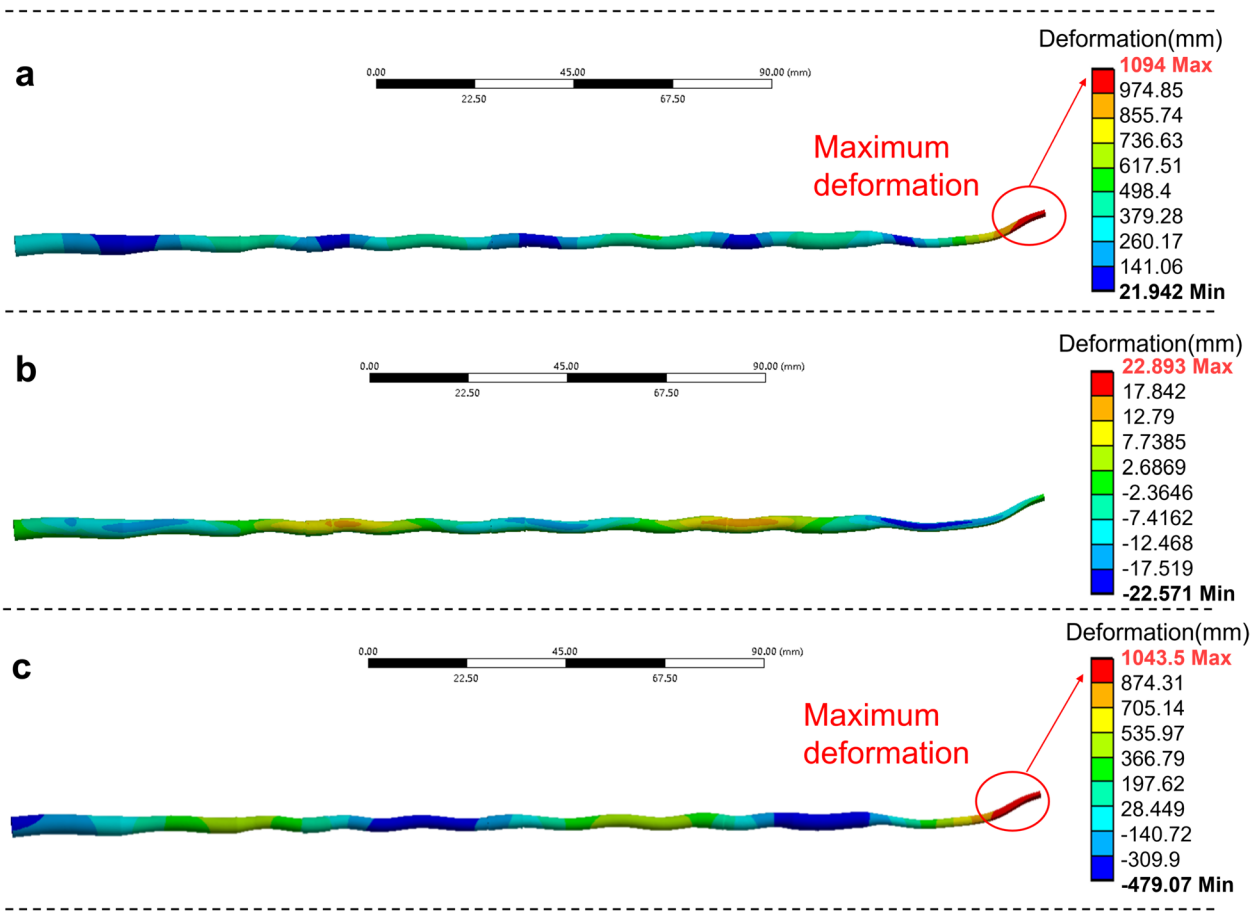

Figure 9 Deformation results of the designed ultrasonic scalpel at 54910 Hz: (**a**) Total deformation, (**b**) Deformation along the *Z* direction, (**c**) Deformation along the *X* direction

of the designed ultrasonic scalpel is five and a half wavelengths, which means it takes 2.5 cycles in total to realize the ultrasonic transmission of the entire ultrasonic scalpel. To facilitate the calculation, the time of an analysis step was set as 5 cycles (9.09×10^{-5} s). According to the linear cumulative damage law, the fatigue life of the ultrasonic scalpel is calculated as the product of the fatigue cycles analyzed by the nCode simulation and the time of an analysis step.

To improve the evaluation of the fatigue life of the designed ultrasonic scalpel, this study compares its performance with that of the Ethicon ultrasonic scalpel, and analyzes the effect of the length of the ultrasonic scalpel rod on the fatigue life. The lengths of the ultrasonic scalpel rod used in different operations are 178 mm, 223 mm, 267 mm, and 401 mm. To obtain a more comprehensive conclusion, the impact of the ultrasonic scalpel rod length on fatigue life is analyzed, and the results are presented in Figure 10. The fatigue life of the ultrasonic scalpel increases as the length of the ultrasonic scalpel rod increases, under the same conditions. Based on this

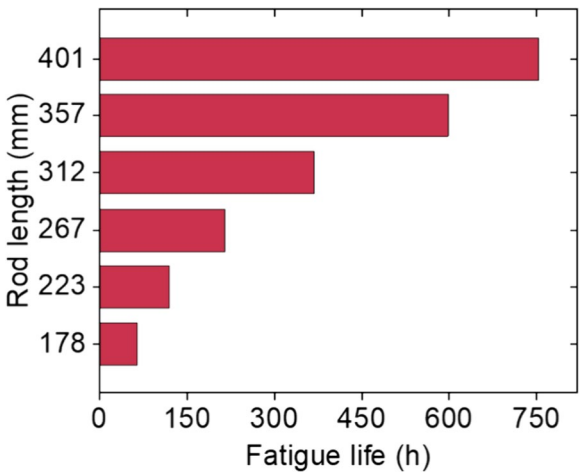

Figure 10 Influence of length of ultrasonic scalpel rod on fatigue life

conclusion, the fatigue life of the Ethicon ultrasonic scalpel and the designed ultrasonic scalpel is compared, and the results are presented in Figure 11. The length and

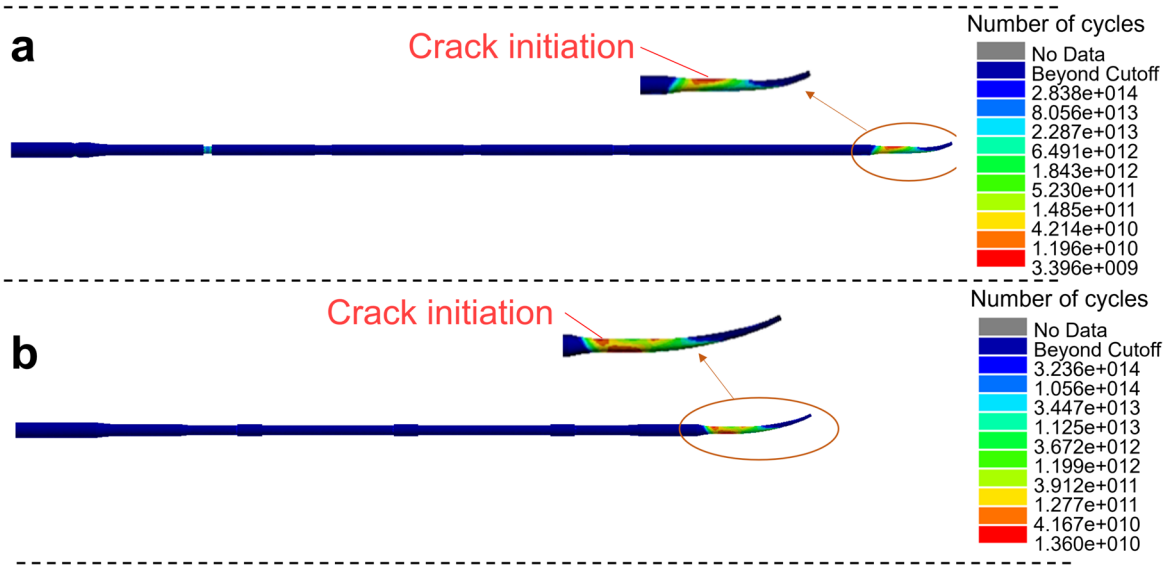

Figure 11 Fatigue simulation results of ultrasonic scalpel: (**a**) Ethicon ultrasonic scalpel, (**b**) Improved ultrasonic scalpel

diameter of the blade of the Ethicon ultrasonic scalpel are the same as those of the blade designed in this study. The maximum damage occurs at the end tip contact area of the gain structure, the Ethicon ultrasonic scalpel has a maximum fatigue cycle count of 3.396×10^9, compared to 1.36×10^{10} for the designed ultrasonic scalpel. Through calculation, the fatigue life of the Ethicon ultrasonic scalpel (under no-load condition and not touching soft tissue) is 366768 s, i.e., 101.88 h, while that of the designed ultrasonic scalpel is 1221000 s, i.e., 340 h. Therefore, the designed ultrasonic scalpel has a better fatigue life.

4 Experimental Investigation on Impedance and Cutting Performance

To verify the cutting ability and impedance characteristics of the designed ultrasonic scalpel, an experimental platform was constructed as illustrated in Figure 12. This platform comprises a digital ultrasonic driver, a processor, an ultrasonic transducer, and the designed ultrasonic scalpel. The ultrasonic driver can measure the impedance, track the resonant frequency, and apply driving voltage to the ultrasonic scalpel. The impedance characteristic curve of the designed ultrasonic scalpel is presented in Figure 13. The processed ultrasonic scalpel has a resonance frequency of 54701 Hz, an antiresonance frequency of 54810 Hz, and an error of only 0.3%, satisfying the design requirements.

To assess the cutting performance of the designed ultrasonic scalpel, fresh liver tissue was selected for experimentation. The built experimental platform was used to perform multiple rounds of cutting at the same position on the liver tissue surface under ± 200 V AC voltage to create a large incision and peel off. The experimental results are shown in Figure 14. The incision was large and deep, and only a small number of fine scorch marks were found upon observing the cross-sectional view, indicating a low degree of damage to the tissues. These results demonstrate that the ultrasonic scalpel possesses basic cutting capability.

5 Conclusions

This study introduced an ultrasonic scalpel with improved service life and presented the optimal design methods for its longitudinal vibration frequency, output amplitude, and fatigue life. The regularity of ultrasonic scalpel design was summarized, and these findings can serve as a reference for the design of future ultrasonic scalpels. The work and conclusions of this study were summarized as follows:

(1) Using a combination of theoretical formula calculation and FEM simulation, the propagation characteristics of ultrasonic waves in a thin rod are investigated, the change rule of the waveform and the positions of the nodes and the antinodes are summarized, and the design method of the amplitude gain of the ultrasonic scalpel is proposed.
(2) A slender, large-curved ultrasonic scalpel tip is designed, and two methods for reducing the stress on the ultrasonic scalpel are proposed. The first way is to set the transition fillet in the gain structure. Through simulation, it is found that the most suitable transition fillet radius is set at 10–20 mm. The

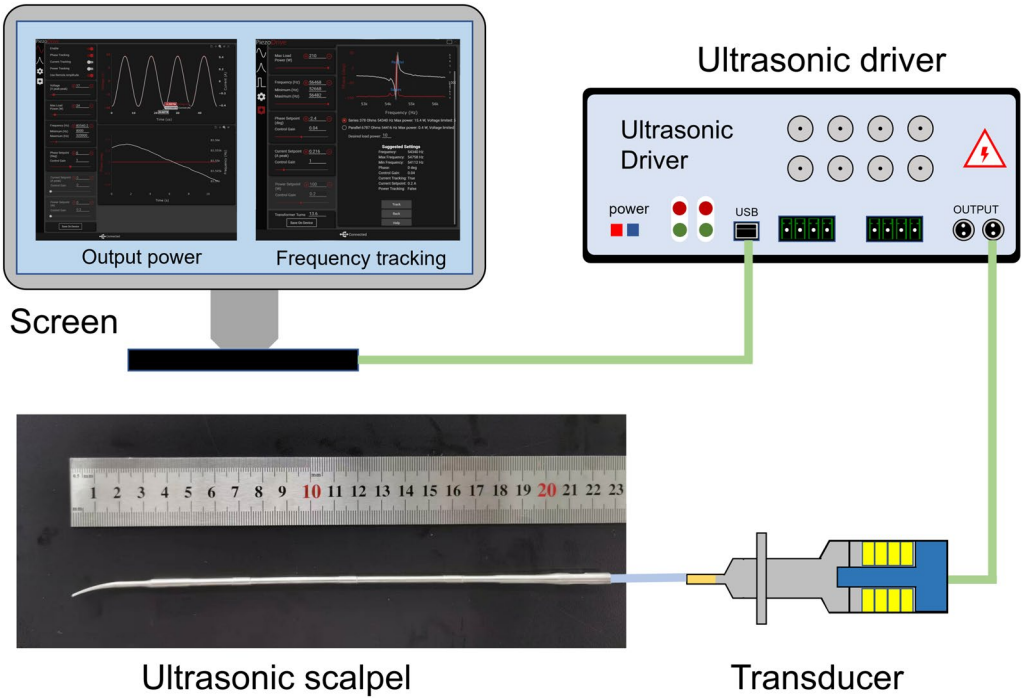

Figure 12 Experimental setup of performance investigation of the presented ultrasonic scalpel

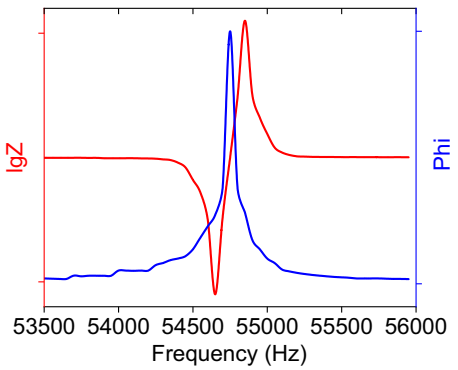

Figure 13 Impedance characteristics of designing ultrasonic scalpel

other way is to extend the end tip by keeping the gain structure away from the node position. Both methods reduce stress and extend the service life of the ultrasonic scalpel effectively.

(3) A frequency adjustment method is proposed, that is, setting VN bosses at the node position or setting VA grooves at the antinode position. Through simulation and comparison, the influence mechanism of the two methods on the resonance frequency and fatigue life of the ultrasonic scalpel is obtained. And a universal conclusion is analyzed, which can realize the multi-objective optimization design of the ultrasonic scalpel.

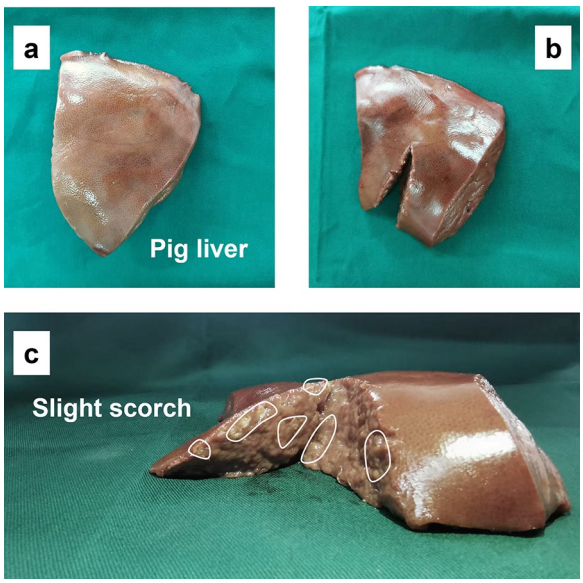

Figure 14 Liver tissue cutting experiment: (**a**) The liver tissue, (**b**) The liver tissue was cut with the designed ultrasonic scalpel, (**c**) Cross-sectional view of liver tissue that has been cut for multiple times

(4) An optimized ultrasonic scalpel was designed and completed, and its vibration performance was verified by model analysis. Through fatigue life simulation, it was demonstrated that the designed ultra-

sonic scalpel had a higher fatigue life compared with the Ethicon ultrasonic scalpel. In addition, the results of impedance measurement experiments and liver tissue cutting experiments show that the designed ultrasonic scalpel has good impedance characteristics and satisfactory cutting performance.

Acknowledgements
Not applicable.

Authors' Contributions
WB was in charge of the whole trial; JZ, RC, DW and GH wrote the manuscript; YZ, XJ, ND and KL assisted with sampling and laboratory analyses. All authors read and approved the final manuscript.

Funding
Supported by National Natural Science Foundation of China (Grant Nos. 52005199, 42241149), Shenzhen Fundamental Research Program of China (Grant Nos. JCYJ20200109150425085, JCYJ20220818102601004), Knowledge Innovation Program of Wuhan-Basic Research of China (Grant No. 2022010801010203), and Shenzhen Science and Technology Program of China (Grant Nos. JSGG20201103100001004, JSGG20220831105800001).

Data Availability
Data will be made available on request.

Declarations

Competing Interests
The authors declare no competing financial interests.

Received: 2 April 2023 Revised: 1 July 2024 Accepted: 8 July 2024
Published online: 01 August 2024

References

[1] Y Gan, B Meng, Y Chen, et al. An intelligent measurement method of the resonant frequency of ultrasonic scalpel transducers based on PSO-BP neural network. *Measurement*, 2022, 190.
[2] L F Grochola, R Vonlanthen. *Surgical energy devices or devices for hemostasis*. In: *Atlas of upper gastrointestinal and hepato-pancreato-biliary surgery*. Heidelberg: Springer, 2016: 37–44.
[3] A Shabbir, D Dargan. Advancement and benefit of energy sealing in minimally invasive surgery. *Asian Journal of Endoscopic Surgery*, 2014, 7(2): 95–101.
[4] C Choi, I G Do, T Song. Ultrasonic versus monopolar energy-based surgical devices in terms of surgical smoke and lateral thermal damage (ULMOST): A randomized controlled trial. *Surgical Endoscopy*, 2018, 32(11): 4415–4421.
[5] D K Dutta, I Dutta. The harmonic scalpel. *The Journal of Obstetrics and Gynecology of India*, 2016, 66(3): 209–210.
[6] T A Emam, A Cuschieri. How safe is high-power ultrasonic dissection? *Annals of Surgery*, 2003, 237(2): 186.
[7] C Shi, D K Luu, Q Yang, et al. Recent advances in nanorobotic manipulation inside scanning electron microscopes. *Microsystems & Nanoengineering*, 2016, 2(1): 1–16.
[8] H Hu, X Zhu, C Wang, et al. Stretchable ultrasonic transducer arrays for three-dimensional imaging on complex surfaces. *Science Advances*, 2018, 4(3): 3979.
[9] A Abdullah, M Shahini, A Pak. An approach to design a high power piezoelectric ultrasonic transducer. *Journal of Electroceramics*, 2009, 22(4): 369–382.
[10] C P Crispi, Jr C P Crispi, Jr P S Silva Reis, et al. Hemostasis with the ultrasonic scalpel. *Journal of the Society of Laparoendoscopic Surgeons*, 2018, 22(4): e2018.00042
[11] J Li, X Dong, S Wang, et al. A novel ultrasonic scalpel rod with multi-stage gain and minification structures for minimally invasive surgery. *2020 IEEE International Conference on Mechatronics and Automation (ICMA)*, Beijing, China, October 13–16, 2020: 1739–1744.
[12] R Cleary, X Li, M Lucas. Incorporating direct metal laser sintered complex shaped Ti-6Al-4V components in ultrasonic surgical devices. *The Journal of the Acoustical Society of America*, 2021, 150(3): 2163–2173.
[13] I Nonaka, S Setowaki, Y Ichikawa. Effect of load frequency on high cycle fatigue strength of bullet train axle steel. *International Journal of Fatigue*, 2014, 60: 43–47.
[14] Y Umehara, M K Kurosawa. A micro ultrasonic scalpel using hydrothermal PZT thin film. *2006 15th IEEE International Symposium on the Applications of Ferroelectrics*, NC, USA, July 30–August 2, 2006: 340–343.
[15] H Wiksell, H Martin, H Coakham, et al. Miniaturised ultrasonic aspiration handpiece for increased applicability. *European Journal of Ultrasound*, 2000, 11(1): 41–46.
[16] J Li, X Dong, G Zhang, et al. An enhanced hemostatic ultrasonic scalpel based on the longitudinal-torsional vibration mode. *IEEE Access*, 2021, 9: 10951–10961.
[17] R W Timm, R M Asher, K R Tellio, et al. Sealing vessels up to 7 mm in diameter solely with ultrasonic technology. *Medical Devices: Evidence and Research*, 2014, 7: 263–271.
[18] J Milsom, K Trencheva, S Monette, et al. Evaluation of the safety, efficacy, and versatility of a new surgical energy device (THUNDERBEAT) in comparison with Harmonic ACE, LigaSure V, and EnSeal devices in a porcine model. *Journal of Laparoendoscopic & Advanced Surgical Techniques*, 2012, 22(4): 378–386.
[19] S C Tjong, G S Wang. High cycle fatigue response of in-situ Al-based composites containing TiB_2 and Al_2O_3 submicron particles. *Composites Science and Technology*, 2005, 65(10): 1537–1546.
[20] S Zhang, Z Chen, H Wu, et al. Bone cutting processes and removal behaviors in orthopedic surgery with an ultrasonic orthopedic scalpel. *Ultrasonics*, 2023, 131: 106966.
[21] S C Tjong, G S Wang. High-cycle fatigue properties of Al-based composites reinforced with in situ TiB_2 and Al_2O_3 particulates. *Materials Science and Engineering*, 2004, 386(1-2): 48-53.
[22] S E Stanzl–Tschegg, H R Mayer, E K Tschegg. High frequency method for torsion fatigue testing. *Ultrasonics*, 1993, 31(4): 275–280.
[23] M Lucas, A MacBeath, E McCulloch, et al. A finite element model for ultrasonic cutting. *Ultrasonics*, 2006, 44: e503–e509.
[24] C Bathias, L Drouillac, P Le Francois. How and why the fatigue S-N curve does not approach a horizontal asymptote. *International Journal of Fatigue*, 2001, 23: 143–151.
[25] R Ebara. Long-term corrosion fatigue behaviour of structural materials. *Fatigue & Fracture of Engineering Materials & Structures*, 2002, 25(8–9): 855–859.
[26] W Li, H Q Zhao, A Nehila, et al. Very high cycle fatigue of TC4 titanium alloy under variable stress ratio: Failure mechanism and life prediction. *International Journal of Fatigue*. 2017, 104: 342–354.
[27] Li B, Wen H, Ye S, et al. Ncode based fatigue life simulation of single cylinder nailer. *International Core Journal of Engineering*, 2022, 8(4): 326–336.
[28] G X Zhang, G G Niu, S S Guo. Analysis of fatigue life of a torsion beam based on nCode design-life. *IOP Conference Series. Materials Science and Engineering*, 2018, 423(1). https://doi.org/10.1088/1757-899X/423/1/012034
[29] F CAO, W Yang, W Zhao, et al. Optimization design of ultrasonic scalpel based on resonant frequency calibration. *The First Graduate Forum of CSAA and the 7th International Academic Conference for Graduates of NUAA*, Nanjing, China, Nov 21–22, 2019: 124–129.
[30] J Chen, F Chen. Design and optimization of a half-wavelength ultrasonic bone scalpel. *Journal of Physics: Conference Series. IOP Publishing*, 2023, 2459(1): 012096.
[31] F R Li, T Y Wang. Optimization experiment of ultrasonic scalpel based on finite element analysis. *Proceedings of the 2022 2nd International Conference on Control and Intelligent Robotics*, Nanjing, China, June, 2022: 316–320.

[32] G P Gavin, G B McGuinness, F Dolan, et al. Performance characteristics of a therapeutic ultrasound wire waveguide apparatus. *International Journal of Mechanical Sciences*, 2007, 49(3): 298–305.
[33] W S Ong, M H Zainulabidin. Vibration characteristics of beam structure attached with vibration absorbers at its vibrational node and antinode by finite element analysis. *JSE Journal of Science and Engineering*, 2020, 1(1): 7–16.
[34] J J Mao, Y J Wang, W Zhang, et al. Vibration and wave propagation in functionally graded beams with inclined cracks. *Applied Mathematical Modelling*, 2023, 118: 166–184.
[35] M Kohantorabi, A H Hemmasi, M Poor Talaei, et al. The study of joints in Oak wood beam compared to the location of node and antinode of longitudinal vibration. *Iranian Journal of Wood and Paper Science Research*, 2021, 36(3): 256–263.
[36] L Wang, Y Liu, J Li, et al. Indirect measurement method of ultrasonic bone cutting force based on antinode vibration displacement. *Journal of Sound and Vibration*, 2023, 552: 117637.
[37] V E Panin, N S Surikova, A M Lider, et al. Multiscale mechanism of fatigue fracture of Ti-6A1-4V titanium alloy within the mesomechanical space-time-energy approach. *Physical Mesomechanics*, 2018, 21: 452–463.
[38] I P Semenova, A V Polyakov, M V Pesin, et al. Strength and fatigue life at 625 K of the Ultrafine-Grained Ti-6Al-4V alloy produced by equal-channel angular pressing. *Metals*, 2022, 12(8): 1345.
[39] H S Zhou, X F Xu, X Cheng, et al. Optimization design of ultrasonic scalpel. *Acoustic Technology*, 2012, 31(1): 48–52.
[40] Y Fu, S Sun, Z Wang, et al. Piezoelectric micromachined ultrasonic transducer with superior acoustic outputs for pulse-echo imaging application. *IEEE Electron Device Letters*, 2020, 41(10): 1572–1575.

Jiaqi Zhao is currently a master candidate at *School of Mechanical and Electronic Information, China University of Geosciences, China*.

Yuhao Zhai is currently a master candidate at *School of Mechanical and Electronic Information, China University of Geosciences, China*.

Xuzhe Jia is currently a master candidate at *School of Mechanical and Electronic Information, China University of Geosciences, China*.

Naiwen Deng is currently a master candidate at *School of Mechanical and Electronic Information, China University of Geosciences, China*.

Kunxu Li is currently a master candidate at *School of Mechanical and Electronic Information, China University of Geosciences, China*.

Guangchao Han is currently a professor at *School of Mechanical and Electronic Information, China University of Geosciences, China*.

Rong Chen is currently a professor at *School of Mechanical and Electronic Information, China University of Geosciences, China*.

Dong Wang is currently a lecturer at *College of Engineering, Mathematics and Physical Sciences, University of Exeter, UK*.

Wei Bai is currently a professor at *School of Mechanical and Electronic Information, China University of Geosciences, China*. His research interests include field-assisted manufacturing theory and ultrasonic-assisted machining.